On-Line Estimation of Rotor Variables in Predictive Current Controllers: A Case Study Using Five-Phase Induction Machines

Jorge Rodas, *Member, IEEE*, Federico Barrero, *Senior Member, IEEE*, Manuel R. Arahal, *Member, IEEE*, Cristina Martín, and Raúl Gregor

Abstract—Predictive current control has been recently proposed like an alternative to conventional PI-PWM current control techniques. Implemented solutions are based on inaccurate estimation of the rotor electrical variables to reduce the computational cost of the method. In this work, the utility and computational cost of predictive current control with different methods for the on-line estimation of the rotor variables are studied. Experimental results are provided to characterize the obtained benefits and drawbacks, using a five-phase induction machine as a case example.

Index Terms—Multiphase induction machine, predictive control, on-line estimation.

Nomenclature

L_{ls}, L_{lr}	Stator/rotor leakage inductance.
L_s, L_r	Stator/rotor inductance.
M	Mutual inductance.
p	Number of pole pairs.
R_s, R_r	Stator/rotor resistance.
T_e	Electromagnetic torque.
T_L	Load torque.
v_{js}	Stator phase j voltage.
i_{js}, i_{jr}	Stator/rotor phase j current.
$u_{\alpha s}$, $u_{\beta s}$	Stator voltages in the $\alpha - \beta$ sub-space.
u_{xs}, u_{ys}	Stator voltages in the $x - y$ sub-space.
u_{zs}	Stator voltages in the z sub-space.
$\psi_{\alpha s}$, $\psi_{\beta s}$	Stator fluxes in the $\alpha - \beta$ sub-space.
$i_{\alpha s}$, $i_{\beta s}$	Stator currents in the $\alpha - \beta$ sub-space.
$i_{\alpha r}$, $i_{\beta r}$	Rotor currents in the $\alpha - \beta$ sub-space.
i_{ds}, i_{qs}	Synchronous stator $d - q$ current components.
ω_r	Rotor electrical speed.
ω_n	Nominal speed.
Vdc	DC-link voltage.
ϑ	Angle between machine phases.
S_i	Switching state, phase i.
J_m	Inertia coefficient.
B_m	Friction coefficient.
$\varpi(t)$	Process noise.
$\nu(t)$	Measurement noise.
Q_ϖ	Covariance matrix of the process noise.
R_ν	Covariance matrix of the measurement noise.
$\mathbf{T}$	Transformation matrix.
$\mathbf{K}$	Kalman filter gain matrix.
$\mathbf{L}$	Luenberger gain matrix.
$\mathbf{H}$	Noise weight matrix.

J. Rodas and R. Gregor are with the Laboratory of Power and Control Systems, Facultad de Ingeniería, Universidad Nacional de Asunción, 2060 Luque, Paraguay (e-mail: jrodas@ing.una.py; rgregor@ing.una.py).

F. Barrero and C. Martín are with the Department of Electronic Engineering, University of Seville, 41004 Seville, Spain (e-mail: fbarrero@us.es; cmartin15@us.es).

M. R. Arahal is with the Department of Systems Engineering and Automatic Control, University of Seville, 41004 Seville, Spain (e-mail: arahal@us.es).

I. Introduction

MODEL predictive control (MPC) has recently gained the attention of the research community like a control technique in power converters and drives [1]. The main drawback of the method, which requires a model of the real system to produce future predictions, is its computational cost. This is particularly evident with electrical drives, where the estimation of non-measurable rotor state variables must be also generated. On the other hand, the main advantage of the MPC technique lies in the flexibility to define different control criteria, to meet constraint satisfaction and to be applied in systems of different dimensions. Several control schemes based on MPC, including current [2], torque [3] and speed [4] control have recently been successfully implemented, and a recent review on the topic can be found in [5]. Developed control schemes have demonstrated good performance in the current and torque regulation of conventional drives and the development of modern microelectronics devices have recently allowed the implementation of MPC technique in multiphase drives, being by far the predictive current control (PCC) technique the most popular case study [6, 7].

The viability of the PCC method is first evaluated in [2] for an asymmetrical six-phase drive. Afterwards different

PCC methods has been proposed in order to reduce the computational cost of the method [8] or to minimize the generated harmonic content combining the selected voltage vector and a zero vector during a sampling period [9]. This idea is further refined in [10, 11] where a proper pulse width modulation (PWM) scheme is combined with the PCC technique, and a voltage reference that ensures sinusoidal output voltage in the linear modulation region is imposed. The PCC method has been extended to the five-phase induction machine (IM) in [12], where the common mode voltage is also reduced, and in [13], where a detailed comparison between PCC and PI-PWM current control techniques is provided. However, all aforementioned research works reduce the problem of estimating rotor quantities using PCC to a simple backtracking procedure, favoring the implementation of the controller. Although published results show the interest of the applied PCC method, they do not analyze the shortcomings that arise from the simplified estimation method. This issue is tackled in this paper motivated by the fact that MPC performance depends on the accuracy of the predictions.

In the existing literature, the problem of state estimation has appeared in a number of cases related mainly to sensor-less applications. For instance, in [14] a model-reference-adaptive-system speed estimator is used with space vector PWM control of an IM. In [15] a Kalman filter is used in a three-phase machine to estimate speed in a drive without PWM. Disturbance estimation have also prompted the use of observers in [16], where the current of a three-phase voltage source PWM rectifier is controlled by a PCC, and in [17], where an extended state observer is used to estimate the lumped disturbances in speed regulation of a permanent magnet synchronous motor. None of these works deal with the estimation of rotor current as proposed here.

In this work, two well-known methods, a Kalman filter (KF) and a Luenberger observer (LO), are used with PCC to reconstruct the rotor variables. A five-phase IM is used as a case example due to its interest in high reliability and fault tolerance industry applications, providing an excellent benchmark due to its higher computational cost compared with the conventional three-phase case [4]. Moreover, the use of a five-phase IM incorporates two extra degrees of freedom to the control problem (the electrical torque is generated in a primary plane, while these extra degrees of freedom are associated with a secondary plane in relation with electrical losses in the IM). The control action mainly affects the primary plane, but the secondary one is also influenced. The use of observers, as it is proposed in this work, can mitigate this influence, improving the system performance and extending the proposal to conventional n-phase IMs (being n any odd number higher than 3, but not only 5). Notice that the use of KF in the context of the stator current prediction and PCC is presented here for the first time. The KF is tuned using a covariance estimation method while a root locus analysis is used with LO, in both cases to produce estimations of the rotor current that improve the needed stator current predictions for PCC.

The paper is organized as follows. Section II analyzes the five-phase IM, whose understanding is required for the definition of the PCC technique, shown in section III. This last section also introduces the accuracy in the rotor state estimation, where different strategies are presented in relation with the case study. Simulation and experimental results using different PCC techniques are compared in section IV, where the interest of using rotor current observers is shown. Finally, the conclusions are summarized in the last section.

II. THE FIVE-PHASE IM

The studied system is a symmetrical five-phase IM with distributed and equally displaced ($\vartheta = 2\pi/5$) windings. A five-phase two-level voltage source inverter (VSI) is used to drive the multiphase machine. The electromechanical system can be modeled considering the standard assumptions of three-phase drives: uniform air gap, sinusoidal magnetomotive force distribution and, negligible core losses and magnetic saturation. The components of the multiphase drive are schematically shown in Fig. 1, where the gating signals that control the multiphase two-level VSI are represented by $[S_a, ..., S_e]$ and their complementary values $[\overline{S}_a, ..., \overline{S}_e]$, being $S_i \in \{0, 1\}$. Then, following the vector space decomposition (VSD) approach [18], four independent variables appear in the system divided into two orthogonal planes called $\alpha - \beta$ and $x - y$, which groups different harmonic components. The harmonic components that contribute to the electromechanical energy conversion are mapped in the $\alpha - \beta$ plane, while $x - y$ components do not generate electrical torque in our case study. An additional axis named z also appears in relation with the zero-sequence component of the system. Stator phase voltages ($\mathbf{v}_s = [v_{as}\ v_{bs}\ v_{cs}\ v_{ds}\ v_{es}]^T$) in normal operation are obtained from the gating signals and the DC-link voltage as it is stated in (1), being detailed in (2) the VSD transformation matrix that defines the stator voltage vectors ($\mathbf{u}_s$) in the $\alpha - \beta$ and $x - y$ planes in (3). Fig. 2 shows the discrete nature of the VSI with a total number of $2^5 = 32$ different switching states and stator voltage vectors in the $\alpha - \beta$ and $x - y$ planes.

$$\mathbf{v}_s = \frac{Vdc}{5} \begin{bmatrix} 4 & -1 & -1 & -1 & -1 \\ -1 & 4 & -1 & -1 & -1 \\ -1 & -1 & 4 & -1 & -1 \\ -1 & -1 & -1 & 4 & -1 \\ -1 & -1 & -1 & -1 & 4 \end{bmatrix} \begin{bmatrix} S_a \\ S_b \\ S_c \\ S_d \\ S_e \end{bmatrix} \quad (1)$$

$$\mathbf{T} = \frac{2}{5} \begin{bmatrix} 1 & \cos(\vartheta) & \cos(2\vartheta) & \cos(3\vartheta) & \cos(4\vartheta) \\ 0 & \sin(\vartheta) & \sin(2\vartheta) & \sin(3\vartheta) & \sin(4\vartheta) \\ 1 & \cos(2\vartheta) & \cos(4\vartheta) & \cos(\vartheta) & \cos(3\vartheta) \\ 0 & \sin(2\vartheta) & \sin(4\vartheta) & \sin(\vartheta) & \sin(3\vartheta) \\ \frac{1}{2} & \frac{1}{2} & \frac{1}{2} & \frac{1}{2} & \frac{1}{2} \end{bmatrix} \quad (2)$$

$$\mathbf{u}_s = \begin{bmatrix} u_{\alpha s} & u_{\beta s} & u_{xs} & u_{ys} & u_{zs} \end{bmatrix}^T = \mathbf{T}\,\mathbf{v}_s \quad (3)$$

Applying the transformation matrix, the mathematical model of the five-phase induction drive can be written using the state-space representation form as follows:

$$\frac{d}{dt}\mathbf{X}(t) = \mathbf{A}\mathbf{X}(t) + \mathbf{B}\mathbf{U}(t) + \mathbf{H}\varpi(t) \quad (4)$$

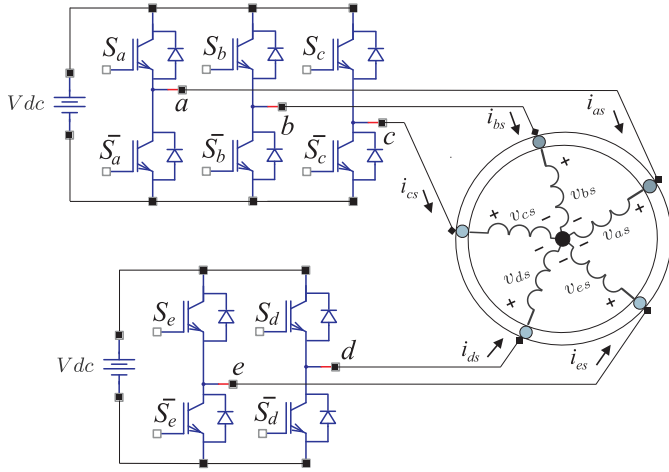$$\mathbf{Y}(t) = \mathbf{C}\mathbf{X}(t) + \nu(t) \quad (5)$$

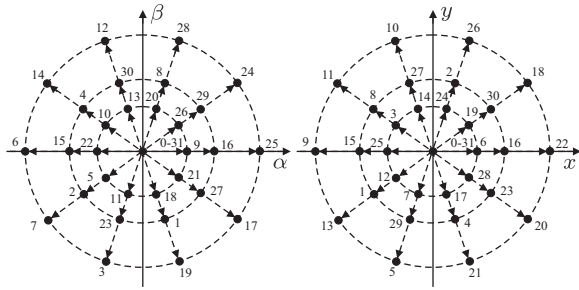Fig. 1. Schematic diagram of the five-phase induction drive.

Fig. 2. Stator voltage vectors and switching states in the $\alpha - \beta$ and $x - y$ sub-spaces for a five-phase symmetrical IM. The number that defines every voltage vector is the decimal value equivalent to the binary $[S_a, \ldots, S_e]$.

$$\mathbf{A} = \begin{pmatrix} -a_{s2} & a_{m4} & 0 & 0 & a_{r4} & a_{l4} \\ -a_{m4} & -a_{s2} & 0 & 0 & -a_{l4} & a_{r4} \\ 0 & 0 & -a_{s3} & 0 & 0 & 0 \\ 0 & 0 & 0 & -a_{s3} & 0 & 0 \\ a_{s4} & -a_{m5} & 0 & 0 & -a_{r5} & -a_{l5} \\ a_{m5} & a_{s4} & 0 & 0 & a_{l5} & -a_{r5} \end{pmatrix} \quad (6)$$

$$\mathbf{B} = \begin{pmatrix} c_2 & 0 & 0 & 0 \\ 0 & c_2 & 0 & 0 \\ 0 & 0 & c_3 & 0 \\ 0 & 0 & 0 & c_3 \\ -c_4 & 0 & 0 & 0 \\ 0 & -c_4 & 0 & 0 \end{pmatrix} \quad (7)$$

with state vector $\mathbf{X}(t) = [i_{\alpha s}\ i_{\beta s}\ i_{xs}\ i_{ys}\ i_{\alpha r}\ i_{\beta r}]^T$, input vector $\mathbf{U}(t) = [u_{\alpha s}\ u_{\beta s}\ u_{xs}\ u_{ys}]^T$ and output vector $\mathbf{Y}(t) = [i_{\alpha s}\ i_{\beta s}\ i_{\alpha r}\ i_{\beta r}]^T$. The coefficients of the matrix $\mathbf{A}$ are defined as $a_{s2} = R_s c_2$, $a_{s3} = R_s c_3$, $a_{s4} = R_s c_4$, $a_{r4} = R_r c_4$, $a_{r5} = R_r c_5$, $a_{l4} = L_r c_4 \omega_r$, $a_{l5} = L_r c_5 \omega_r$, $a_{m4} = M c_4 \omega_r$ and $a_{m5} = M c_5 \omega_r$ with coefficients c_i defined as $c_1 = L_s L_r - M^2$, $c_2 = \frac{L_r}{c_1}$, $c_3 = \frac{1}{L_{ls}}$, $c_4 = \frac{M}{c_1}$, $c_5 = \frac{L_s}{c_1}$. The

electromagnetic torque of the drive can be obtained from the following equation:

$$T_e = \frac{5}{2} p \left(\psi_{\alpha s} i_{\beta s} - \psi_{\beta s} i_{\alpha s} \right) \quad (8)$$

Finally, the relationship between the torque and the rotor electrical speed can be written as:

$$J_m \frac{d}{dt} \omega_r + B_m \omega_r = p \left(T_e - T_L \right) \quad (9)$$

These equations are the basis for the PCC method, as will be shown in the next section.

III. PCC IN SYMMETRICAL FIVE-PHASE IM: ACCURACY IN THE ROTOR STATE ESTIMATION

The research activity in the last years in the multiphase drives' field has focused, mainly, in asymmetrical six-phase and symmetrical five-phase IM with sinusoidally distributed stator windings. Sophisticated control solutions have been proposed to enhance torque generation, to improve the overall system performance and to reduce the stator current harmonic injection [6]. MPC has been proposed in [3], as a competitor of direct torque control, for the torque control of a five-phase IM drive. However, it has been more commonly used in conjunction with the rotor-flux oriented control (RFOC) method substituting the inner PI-PWM stator current closed loop [13]. In this last work the predictive method is introduced as FCS-MPC in oposition to previous works that use MPC with PWM.

Fig. 3 shows a general scheme of a five-phase variable speed drive using a simple RFOC technique where the inner current control loop can be realized using either PI-PWM or PCC. The basis of the PCC method is the predictive model, obtained from the discretization of the model of the real system, eq. (4)-(7). This model enables the computation of a prediction of the state $(\hat{\mathbf{X}}_{[k+1|k]})$ by means of:

$$\hat{\mathbf{X}}_{[k+1|k]} = f \left(\mathbf{X}_{[k]}, \mathbf{U}_{[k]}, T_m, \omega_{r[k]} \right) \quad (10)$$

where k identifies the actual discrete-time sample, T_m is the sampling time, and $\hat{\mathbf{X}}_{[k+1|k]}$ is a prediction of the future state made at time k. The PCC considers the effect of all possible control actions over the evolution of the state variables, selecting (for application at the next sampling time) the one that better suits the control objectives. It is thus a very general technique as it can incorporate different objectives and constraints.

The PCC results are largely dependent on the accuracy of the predictions, like in other model-based control approaches. In this regard, the use of rotor quantities estimators can help improving the performance as will be shown later.

The evolution of the state variables can be represented using the following equations derived from (10):

$$\begin{bmatrix} \hat{\mathbf{X}}_{a[k+1|k]} \\ \hat{\mathbf{X}}_{b[k+1|k]} \end{bmatrix} = \begin{bmatrix} \overline{\mathbf{A}}_{11} & \overline{\mathbf{A}}_{12} \\ \overline{\mathbf{A}}_{21} & \overline{\mathbf{A}}_{22} \end{bmatrix} \begin{bmatrix} \mathbf{X}_{a[k]} \\ \mathbf{X}_{b[k]} \end{bmatrix} + \begin{bmatrix} \overline{\mathbf{B}}_1 \\ \overline{\mathbf{B}}_2 \end{bmatrix} \mathbf{U}_{\alpha\beta s[k]} \quad (11)$$

$$\mathbf{Y}_{[k]} = \begin{bmatrix} \overline{\mathbf{I}} & \overline{\mathbf{0}} \end{bmatrix} \begin{bmatrix} \mathbf{X}_{a[k]} \\ \mathbf{X}_{b[k]} \end{bmatrix} \quad (12)$$
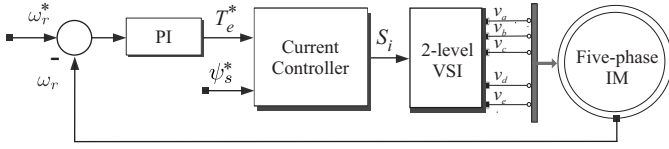
Fig. 3. General scheme of a variable speed drive using a RFOC technique and different inner current controllers.

where $\mathbf{X}_a = \begin{bmatrix} i_{\alpha s[k]} & i_{\beta s[k]} \end{bmatrix}^T$ is a vector containing the measured stator currents in $\alpha - \beta$ axes, $\mathbf{X}_b = \begin{bmatrix} i_{\alpha r[k]} & i_{\beta r[k]} \end{bmatrix}^T$ is the remaining portion of the state, which is not measured and has to be estimated, and $\overline{\mathbf{I}}$ is the identity matrix.

Consequently, the prediction of the stator currents in the fundamental flux and torque production plane (the $\alpha - \beta$ plane) and using the standard PCC solution have a measurable part ($\mathbf{m}_{[k]} = \begin{bmatrix} m_{\alpha[k]} & m_{\beta[k]} \end{bmatrix}^T$), which contains variables such as stator currents, rotor speed and the stator voltages, and a non-measured part ($\mathbf{n}_{[k]} = \begin{bmatrix} n_{\alpha[k]} & n_{\beta[k]} \end{bmatrix}^T$), (ie. rotor currents). Assuming this, the predictive equations can be written as follows:

$$\hat{\mathbf{X}}_{a[k+1|k]} = \mathbf{m}_{[k]} + \hat{\mathbf{n}}_{[k|k]} \qquad (13)$$

Eq. (13) establishes a prediction of the stator currents in the $\alpha - \beta$ sub-space for the $k + 1$ sampling time using the measurements of the k sampling time. Consequently, to solve the equations it is necessary to obtain an accurate estimation of the value of $\hat{\mathbf{n}}_{[k|k]}$, which can be solved using:

$$\hat{\mathbf{n}}_{[k|k]} = \hat{\mathbf{n}}_{[k-1]} = \mathbf{X}_{a[k]} - \mathbf{m}_{[k-1]} \qquad (14)$$

Considering null initial condition $\hat{\mathbf{n}}_{[0]} = 0$, the estimated portion that represents the rotor currents can be calculated from a recursive formula given by:

$$\hat{\mathbf{n}}_{[k|k]} = \hat{\mathbf{n}}_{[k-1]} + (\mathbf{X}_{a[k]} - \hat{\mathbf{X}}_{a[k-1]}) \qquad (15)$$

In PCC the predictive model is computed for each possible voltage vector, as well as the cost function to determine the stator voltage vector that minimizes it (S^{opt}). This cost function gives flexibility to the PCC method, offering different control objectives. We will use in this case study the following cost function:

$$J = |\hat{e}_{\alpha\beta}|^2 + \lambda_{xy}|\hat{e}_{xy}|^2 \qquad (16)$$

where $\hat{e}$ a second-step ahead prediction error computed as $\hat{e} = i^*_{s[k+2|k]} - \hat{i}_{s[k+2|k]}$, and λ_{xy} is a tuning parameter that allows to put more emphasis on $\alpha - \beta$ or $x - y$ sub-spaces, being $x - y$ plane in relation with the machine losses.

The PCC technique is illustrated by Fig. 4. Instead of the backtracking procedure that has been successfully applied in previous research works, the use of different rotor state estimation methods is analyzed here to assess the improvements in estimation accuracy and in control performance.

A. Rotor state estimation based on Kalman filters

The application of KF in electrical systems is not new, but it has not been previously considered with PCC. The KF design considers uncorrelated process and zero-mean Gaussian measurement noises, thus the dynamics of the KF are:

$$\hat{\mathbf{X}}_{b[k+1|k]} = (\overline{\mathbf{A}}_{22} - \mathbf{K}\overline{\mathbf{A}}_{12})\hat{\mathbf{X}}_{b[k]} + \mathbf{K}\mathbf{Y}_{[k+1]} +$$
$$(\overline{\mathbf{A}}_{21} - \mathbf{K}\overline{\mathbf{A}}_{11})\mathbf{Y}_{[k]} + (\overline{\mathbf{B}}_2 - \mathbf{K}\overline{\mathbf{B}}_1)\mathbf{U}_{\alpha\beta s[k]} \qquad (17)$$

being $\mathbf{K}$ the KF gain matrix that is calculated from the covariance of the noises at each sampling time in a recursive manner as:

$$\mathbf{K}_{[k]} = \Gamma_{[k]} \cdot \overline{\mathbf{C}}^T \hat{R}_\nu^{-1} \qquad (18)$$

where Γ is the covariance of the new estimation, which it is defined like a function of the old covariance estimation (φ) as follows:

$$\Gamma_{[k]} = \varphi_{[k]} - \varphi_{[k]} \cdot \overline{\mathbf{C}}^T (\overline{\mathbf{C}} \cdot \varphi_{[k]} \cdot \overline{\mathbf{C}}^T + \hat{R}_\nu)^{-1} \cdot \overline{\mathbf{C}} \cdot \varphi_{[k]} \qquad (19)$$

From the state equation, which includes the process noise, it is possible to obtain a correction of the covariance of the estimated state as:

$$\varphi_{[k+1]} = \overline{\mathbf{A}}\Gamma_{[k]} \cdot \overline{\mathbf{A}}^T + \overline{\mathbf{H}}\hat{Q}_\varpi \cdot \overline{\mathbf{H}}^T \qquad (20)$$

This completes the required relations for the optimal state estimation using KF with PCC. Thus, $\mathbf{K}$ provides the minimum estimation errors, given a knowledge of the process noise magnitude ($\hat{Q}_\varpi$), the measurement noise magnitude ($\hat{R}_\nu$), and the covariance initial condition ($\varphi_{[0]}$).

In this work, the KF is designed using an standard covariance estimation method [19] in which the covariance matrices are computed from prediction errors assuming uncorrelated noise vectors of zero mean. This kind of estimation is biased but at least is supported by data. The proposed rotor current estimator based on KF can be summarized with the pseudocode shown in Algorithm 1. The optimal design of the KF by means of a robust covariance estimation neither is a common subject in the field nor is the purpose of our work, which is mainly focused in a proof of concept study of the rotor state estimation techniques for PCC.

Algorithm 1 KF-based PCC

Compute the covariance matrix.
Compute the KF gain matrix.
$J_o := \infty$, $i := 1$
while $i \leq \varepsilon$ **do**
  $S_i \leftarrow S_i^j \ \forall \ j = 1, \ldots, e$
  Compute stator voltages.
  Compute the prediction of the measurement state.
  Compute the cost function.
  if $J < J_o$ **then**
    $J_o \leftarrow J$, $S^{opt} \leftarrow S_i$
  end if
  $i := i + 1$
end while
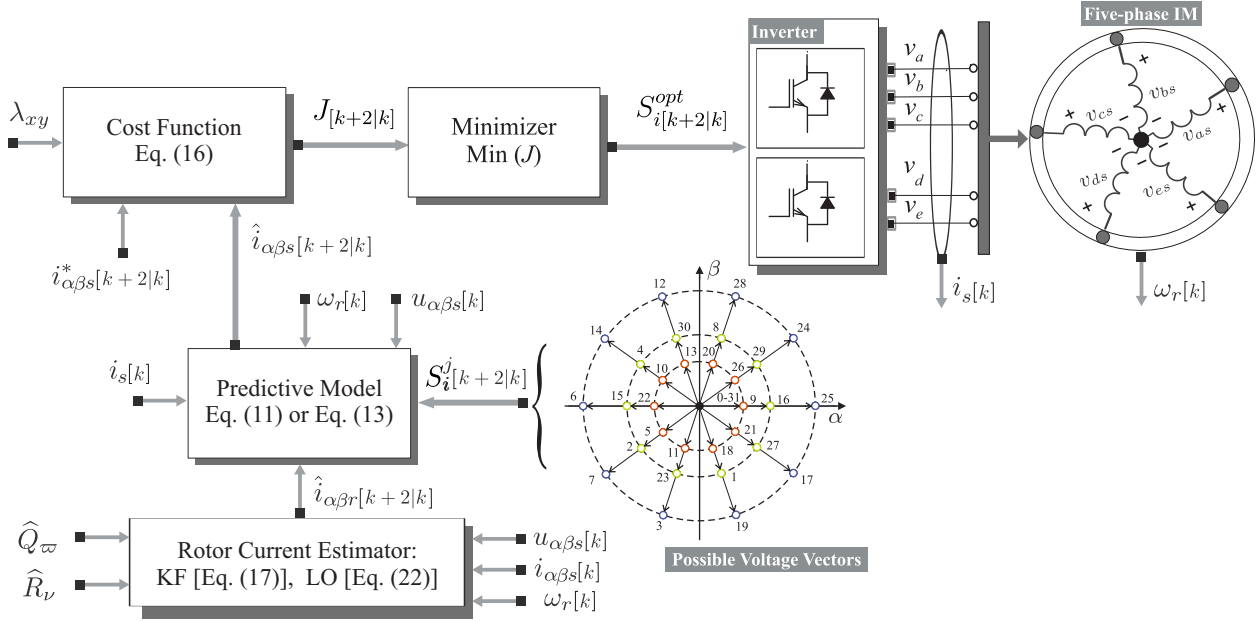Compute the correction for the covariance matrix.

Fig. 4. Proposed PCC techniques with rotor current estimators in symmetrical five-phase IM.

B. Rotor state estimation using Luenberger observers

Observer theory (due mainly to Luenberger) is a well established discipline allowing the design of estimation schemes for different systems. Most observers proposals for IM use the RFOC scheme. In this work, the observer must produce an estimation of two variables: the rotor currents $i_{\alpha r}$ and $i_{\beta r}$. The row rank of the observability matrix equals the systems dimension, allowing an adequate placement of closed loop poles:

$$\hat{\mathbf{X}}_{[k+1]} = \overline{\mathbf{A}}\mathbf{X}_{[k]} + \overline{\mathbf{B}}\mathbf{U}_{[k]} - \mathbf{L}\left(\overline{\mathbf{C}}\mathbf{X}_{[k]} - \mathbf{Y}_{[k]}\right) \quad (21)$$

which are determined by the observer gain $\mathbf{L}$. The convergence towards zero of the estimation error is then determined by the choice of $\mathbf{L}$, and the separation principle allows the choice of such matrix to be decoupled from the controller design, although optimal results are not guaranteed. The dynamic of the LO is modeled by the following equation:

$$\hat{\mathbf{X}}_{b[k+1]} = (\overline{\mathbf{A}}_{22} - \mathbf{L}\overline{\mathbf{A}}_{12})\hat{\mathbf{X}}_{b[k]} + \mathbf{L}\mathbf{Y}_{[k+1]} + \\ (\overline{\mathbf{A}}_{21} - \mathbf{L}\overline{\mathbf{A}}_{11})\mathbf{Y}_{[k]} + (\overline{\mathbf{B}}_2 - \mathbf{L}\overline{\mathbf{B}}_1)\mathbf{U}_{\alpha\beta\mathbf{s}[k]} \quad (22)$$

Where the design stage implies the selection of the most adequate eigenvalues of $(\overline{\mathbf{A}}_{22} - \mathbf{L}\overline{\mathbf{A}}_{12})$. For a fast error convergence to zero, the real parts of those eigenvalues should be as negative as possible. However, the values in the model matrices may not be exactly known. In order for the observer to be robust against modeling errors, it is important that the observer has well-damped dynamics, locating the poles at some distance from the origin with imaginary parts no larger than the real parts. The Luenberger gain matrix can have the usual form:

$$\mathbf{L} = \begin{pmatrix} g_1 & -g_2 \\ g_2 & g_1 \end{pmatrix} \quad (23)$$

where coefficients g_i are derived using the Kautsky-Nichols algorithm [20] to match the desired closed loop observer poles.

The location of the poles is determined by root locus analysis of the open loop system linearized around the operating point. The reader is referred to [21] for more details. Now, as the coefficients of $\overline{\mathbf{A}}_{22}$ are dependent of ω_r it is necessary to solve the pole placement problem for the current value of ω_r. Algorithm 2 shows a pseudocode of the proposed rotor current estimator based on LO.

Algorithm 2 LO-based PCC

> $J_o := \infty$, $i := 1$
> **while** $i \le \varepsilon$ **do**
> $S_i \leftarrow S_i^j \; \forall \, j = 1, \ldots, e$
>   Compute stator voltages.
>   Compute the prediction of the measurement states.
>   Compute the cost function.
>   **if** $J < J_o$ **then**
> $J_o \leftarrow J$, $S^{opt} \leftarrow S_i$
>   **end if**
> $i := i + 1$
> **end while**
> Compute the prediction.

IV. OBTAINED RESULTS

To study the performance of the PCC with different estimation methods (PCC without a proper rotor observer and employing the conventional update and hold technique for estimating the rotor quantities or C1 from now on, PCC with a KF-based rotor current observer or C2, and PCC with a LO-based rotor current observer or C3 in what follows), some experimental tests have been carried out using a laboratory prototype and a 30-slot symmetrical five-phase IM with three pairs of poles (see Fig. 5). The nominal parameters of the machine are detailed in Table I and were obtained through
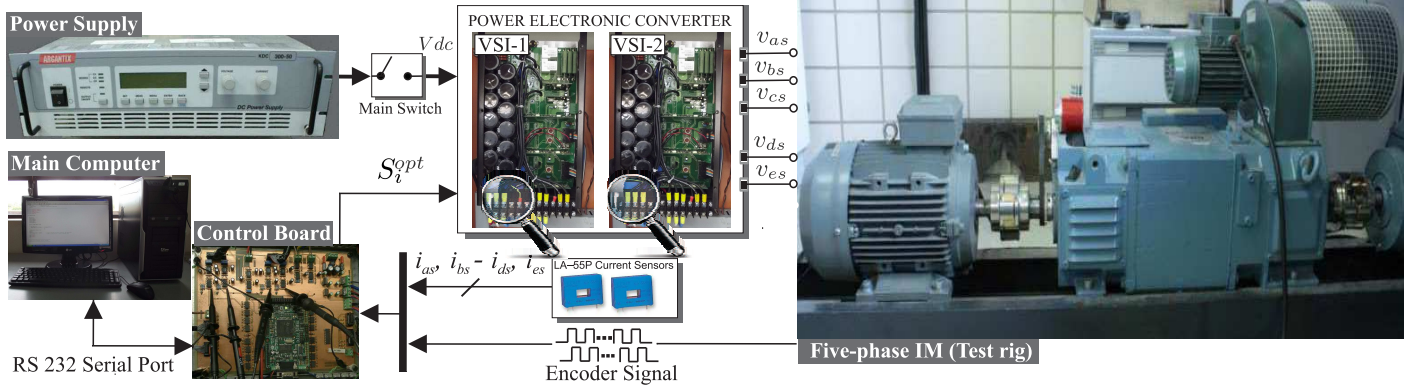
Fig. 5. Scheme of the experimental test rig.

TABLE I
ELECTRICAL AND NOMINAL PARAMETERS OF THE ANALYZED
FIVE-PHASE IM

Parameter	Symbol	Value	Unit
Stator resistance	R_s	19.45	Ω
Rotor resistance	R_r	6.77	Ω
Stator leakage inductance	L_{ls}	100.7	mH
Rotor leakage inductance	L_{lr}	38.6	mH
Mutual inductance	M	656.5	mH
Nominal speed	ω_n	1 000	rpm
Power	P	1	kW
Number of pole pairs	p	3	—

extensive experimentation in [22] and [23]. An independent power supply, which set the DC-Link to 300 V, and two conventional SKS21F power converters from Semikron drive the five-phase machine, while the control system is based on the TM320F28335 Texas Instrument DSP and the MSK28335 Technosoft board. Variable load conditions are applied using a DC machine that it is mechanically coupled to the five-phase IM. The value of the process noise and the measurement noise have been determined by a covariance estimation method as $\widehat{Q}_\varpi = 0.00135$ and $\widehat{R}_\nu = 0.0013$, while the Luenberger gain coefficients have been determined as $g_1 = 0.1400615$ and $g_2 = 1.1424165$. The same sampling frequency, $f_s = 10$ kHz, and cost function defined in (16) with $\lambda_{xy} = 0.1$ are used for C1, C2 and C3, and the steady-state and transient responses of the controlled system are compared. In order to compare quantitatively the different controllers several figures of merit are used. In all cases the root mean square quantity defined in (24) is used.

$$\text{MSE}(W) = \sqrt{\frac{1}{N} \sum_{j=1}^{N} W_j^2} \qquad (24)$$

The figures of merit are the mean squared control errors like the tracking error of the stator current in α and x axes, defined

as $\text{MSE}(i_{\alpha s}^* - i_{\alpha s})$ and $\text{MSE}(i_{xs}^* - i_{xs})$, respectively, and the mean squared prediction error in α axis, defined as $\text{MSE}(\hat{i}_{\alpha s} - i_{\alpha s})$. Please note that α axis is representative of the $\alpha - \beta$ plane, being results for β axis virtually the same. A similar remark can be made regarding the x axis, representing the $x - y$ plane.

First, the steady-state performance of the controlled system using C1, C2 and C3 is studied, as shown in Fig. 6. The use of rotor observers (middle and lower plots) notably improve the system performance in $\alpha - \beta$ and $x - y$ sub-spaces (left and right plots, respectively). As commented before, the response in the β axis that has not been included for the sake of conciseness. The obtained MSE of the stator current in the fundamental flux and torque production plane is reduced by 25.54 % and 28.73 % using C2 and C3 methods, respectively, as it is detailed in Table II. Similar results were obtained using different operation points, as it is also shown in Table II, where the use of rotor state observers improves the steady-state performance of the controlled system, reducing the obtained MSE in the $\alpha - \beta$ sub-space more than 20 % for all analyzed cases. Notice that the aforementioned improvement in the electrical torque production is accompanied with a huge reduction of the electrical losses in the multiphase machine. For example, the obtained MSE in the $x - y$ sub-space at 1.6 A and 25 Hz is reduced by 43.13 % and 42.30 % using C2 and C3 methods, respectively. This improvement is a consequence of a better stator current prediction using C2 and C3 techniques, characterized by the reduction in the MSE of the model prediction error (see Table II). Finally, notice that from the computational cost perspective, one of the main expected drawbacks for the implementation of the proposed PCC methods in industry applications is the required computational load. However, the addition of the rotor current observer produces a manageable increment of the total required computational cost of the controller, being $33.38\mu s$, $52.50\mu s$ and $35.78\mu s$ with C1, C2 and C3 techniques, respectively, with a sampling time of $100\ \mu s$.

A transient test is then realized to evaluate the performance of all PCC controllers. The multiphase machine is managed in the torque operation mode but the reference of the stator
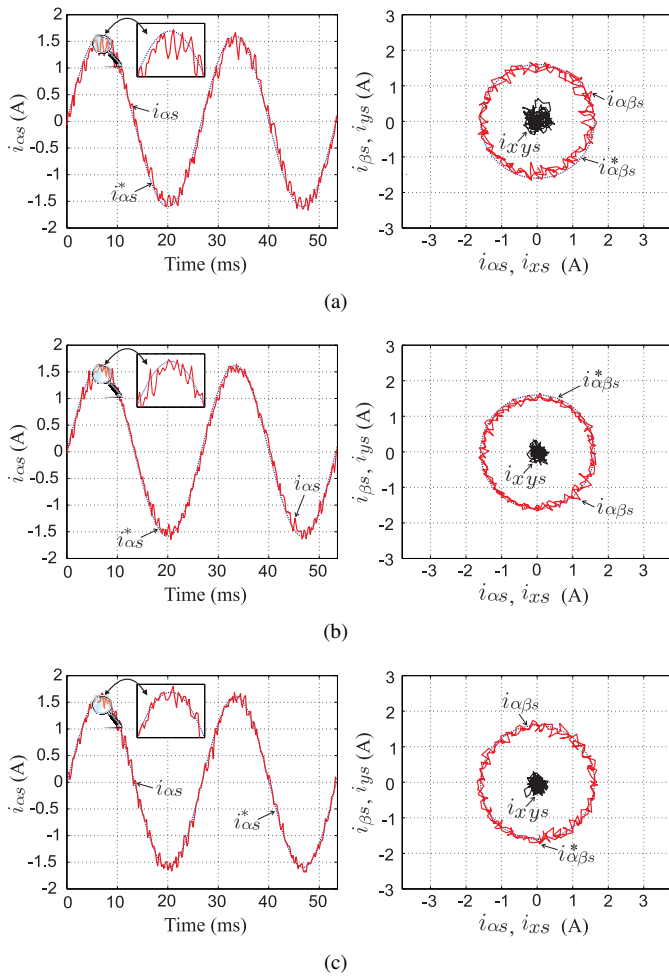
Fig. 6. Performance in steady-state using C1 (a), C2 (b) and C3 (c) control methods for $f_e = 25$ Hz, $i^*_{\alpha\beta s} = 1.6$ A.

TABLE II
COMPARISON OF THE C1, C2 AND C3 PCC METHODS

Steady-state ($i^*_{\alpha\beta s} = 1.6$ A)		Rotor current estimator		
f_e (Hz)	MSE	C1	C2	C3
35	MSE ($i^*_{\alpha s} - i_{\alpha s}$)	0.1517	0.1060	0.1028
	MSE ($\hat{i}_{\alpha s} - i_{\alpha s}$)	0.1994	0.1251	0.1424
	MSE ($i^*_{xs} - i_{xs}$)	0.2223	0.1797	0.2069
25	MSE ($i^*_{\alpha s} - i_{\alpha s}$)	0.1288	0.0959	0.0918
	MSE ($\hat{i}_{\alpha s} - i_{\alpha s}$)	0.1903	0.1351	0.1236
	MSE ($i^*_{xs} - i_{xs}$)	0.2754	0.1566	0.1589
15	MSE ($i^*_{\alpha s} - i_{\alpha s}$)	0.1213	0.0844	0.0971
	MSE ($\hat{i}_{\alpha s} - i_{\alpha s}$)	0.1793	0.1255	0.1146
	MSE ($i^*_{xs} - i_{xs}$)	0.2466	0.1692	0.1612

TABLE III
EXPERIMENTAL RESULTS USING DIFFERENT T_L VALUES AT $f_e = 29$ Hz

T_L (%)	MSE ($i^*_{\alpha s} - i_{\alpha s}$)	MSE ($\hat{i}_{\alpha s} - i_{\alpha s}$)	MSE ($i^*_{xs} - i_{xs}$)
40	0.0829	0.0983	0.0905
60	0.0784	0.1030	0.1010
80	0.0849	0.1190	0.1050

current is continuously changed using a step profile (from a positive electrical torque to a negative one, and viceversa) to force changes in the rotation direction of the machine. This is easily obtained if the stator current in the fundamental flux and torque production $\alpha - \beta$ plane is rotated into the synchronous $d - q$ frame, where i_{ds} is maintained constant and equal to 0.57 A and the sign of i_{qs} is changed from positive to negative and viceversa, using the step profile. Notice that the estimation of the slip factor is performed in the same manner as using indirect RFOC methods. Fig. 7 shows the obtained results, where the stator current responses in $d-q$ and $x-y$ sub-spaces are depicted using C1 (left plots, Fig. 7a), C2 (middle plots, Fig. 7b) and C3 (right plots, Fig. 7c) methods. It can be observed that similar tracking performance is obtained in the q axis using the three techniques, but C1 method introduces a higher detuning effect in the d axis and much worse current tracking in the $x - y$ plane.

In addition, some tests have been carried out in steady-state varying the load torque in the multiphase drive. In this set of experiments the electrical frequency is set to 29 Hz. Fig. 8 summarizes the obtained results, where three different load toque (T_L) values are used (about 40%, 60% and 80% of the nominal one). With respect to the current tracking and prediction errors, the obtained results and conclusions remain the same for all load torque values, validating the performance of the proposal at different load torque conditions and, consequently, different thermal conditions in the copper windings. Table III compares the obtained MSE values of the tracking and control errors of the stator current for considered load torques. It can be noticed that the obtained results using the proposed observer are quite similar, although slightly greater MSE values are obtained with higher load torques in $\alpha - \beta$ and $x - y$ sub-spaces.

A low voltage test is also performed to analyze the effect of non-ideal power converter effects (like deadbeat compensation). Again, the steady-state performance under no-load condition is studied. Fig. 9 shows the obtained results, where it can be appreciated that the controller performs similarly to previous cases (see Fig. 8). In fact, the obtained MSE values of the tracking and control errors in the stator current α axis, MSE($i^*_{\alpha s} - i_{\alpha s}$) and MSE($\hat{i}_{\alpha s} - i_{\alpha s}$) respectively, are 0.1037 A and 0.1001 A, similar to the values obtained in Table III.

To conclude the analysis it is interesting to make a comparison between the estimation of the rotor current provided by the KF and LO techniques. The experimental system does not include the possibility of making rotor currents' measurement. Then, we have made the comparison in simulations, using matlab/simulink and a model of the real test rig and of the used five-phase IM (Table I). Fig. 10 illustrates the obtained results. The obtained results show an accurate agreement between real and estimated current using both estimators. In terms of accuracy KF and LO exhibit excellent performance, which can be concluded from the fact that MSE($\hat{i}_{\alpha r} - i_{\alpha r}$) takes a 0.0192 A value using KF while 0.0194 A for LO. This is in accordance with the observed improvement in PCC current tracking as reported in Table II.
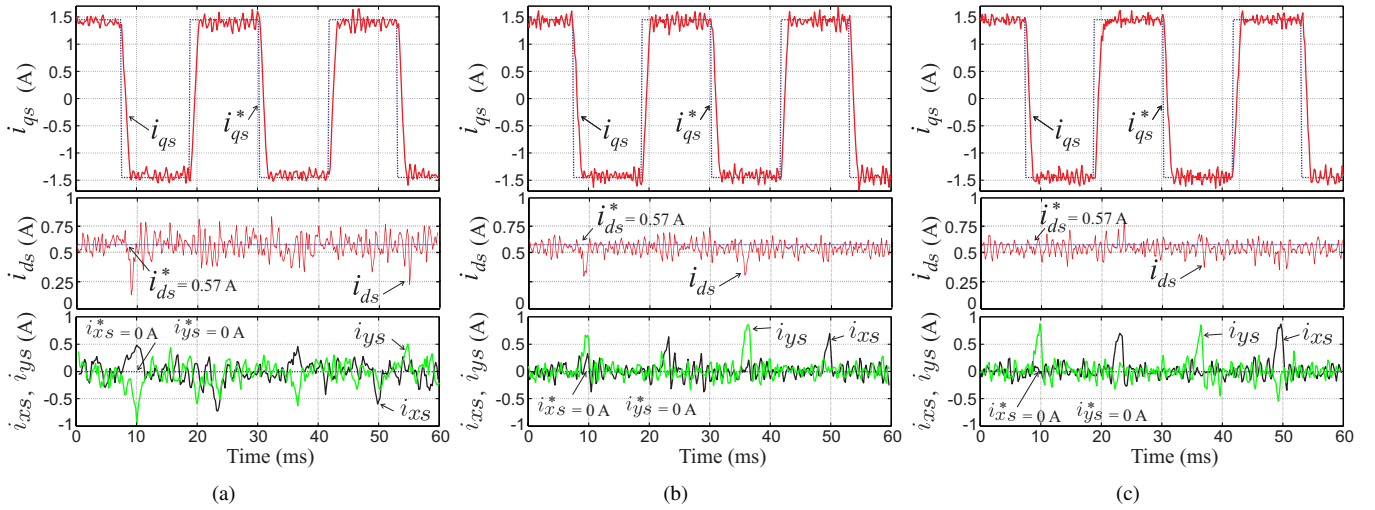
Fig. 7. Performance in transient state. Different steps in the torque stator reference current i_{qs} are applied while the multiphase IM is operated in the torque control mode.
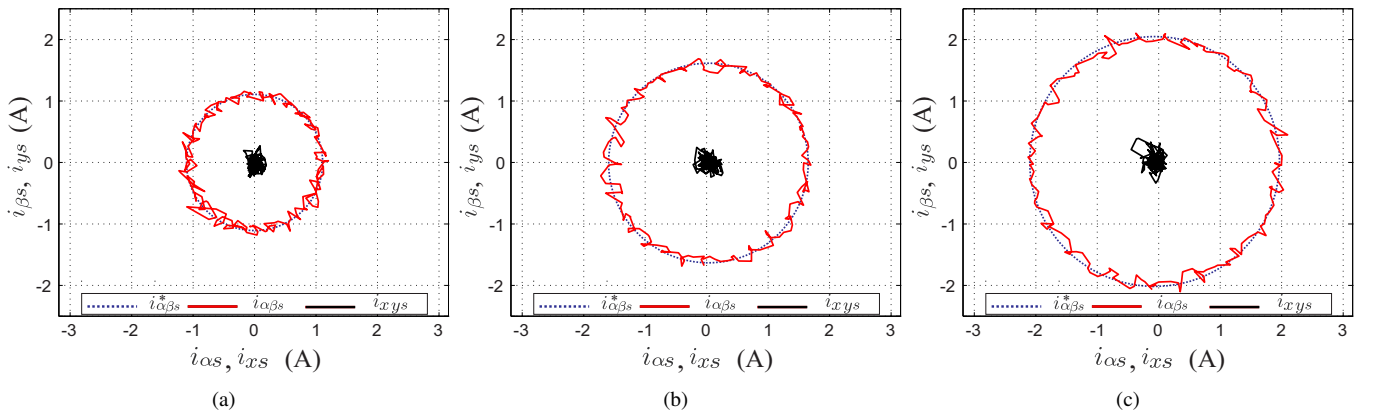

Fig. 8. Performance in steady-state using different load toque values (a) $T_L = 40$ %, (b) $T_L = 60$ % and (c) $T_L = 80$ % at $f_e = 29$ Hz.
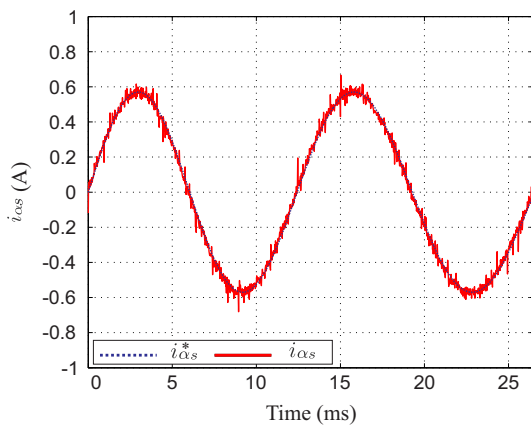

Fig. 9. Stator current in the α axis at low terminal voltages.

Fig. 10. Rotor current estimation results in sinusoidal steady-state using KF and LO control methods.

V. CONCLUSION

This paper addresses for the first time the interest of using estimation methods for the rotor state variables in predictive current controllers. A five-phase IM drive is used as case study since it provides a challenging scenario. Two
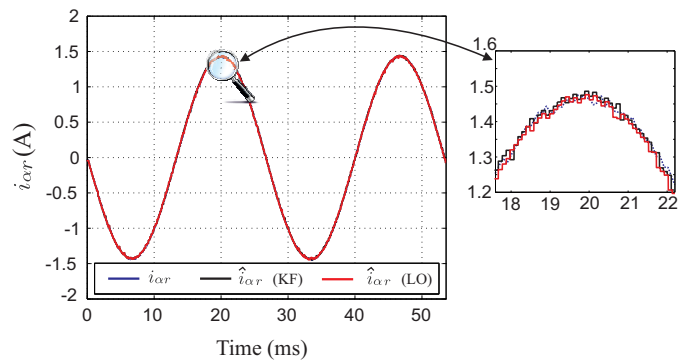
different estimation methods have been used: KF and LO, and the resulting controllers have been compared with the standard PCC approach. The KF has been tuned using a covariance estimation method while a root locus analysis was applied with LO. The obtained experimental results

show that the system performance is improved using rotor state (rotor currents) estimations, which can be relevant in the development of high-performance motor drives because the added computational cost is manageable for modern microelectronic devices.

REFERENCES

[1] J. Rodriguez, M. Kazmierkowski, J. Espinoza, P. Zanchetta, H. Abu-Rub, H. Young and C. Rojas, "State of the art of finite control set model predictive control in power electronics," *IEEE Trans. Ind. Informat.*, vol. 9, no. 2, pp. 1003–1016, 2013.

[2] M.R. Arahal, F. Barrero, S. Toral, M.J. Duran and R. Gregor, "Multi-phase current control using finite-state model-predictive control," *Control Eng. Pract.*, vol. 17, no. 5, pp. 579–587, 2009.

[3] J. Riveros, F. Barrero, E. Levi, M.J. Duran, S. Toral and M. Jones, "Variable-speed five-phase induction motor drive based on predictive torque control," *IEEE Trans. Ind. Electron.*, vol. 60, no. 8, pp. 2957–2968, 2013.

[4] M. Preindl and S. Bolognani, "Model predictive direct speed control with finite control set of PMSM drive systems," *IEEE Trans. Power Electron.*, vol. 28, no. 2, pp. 1007–1015, 2013.

[5] S. Kouro, M.A. Perez, J. Rodriguez, A.M. Llor and H.A. Young, "Model predictive control: MPC's role in the evolution of power electronics," *IEEE Ind. Electron. Mag.*, vol. 9, no. 4, pp. 8–21, 2015.

[6] F. Barrero and M.J. Duran, "Recent advances in the design, modeling and control of multiphase machines – Part 1," *IEEE Trans. Ind. Electron.*, vol. 63, no. 1, pp. 449–458, 2016.

[7] M.J. Duran and F. Barrero, "Recent advances in the design, modeling and control of multiphase machines – Part 2," *IEEE Trans. Ind. Electron.*, vol. 63, no. 1, pp. 459–468, 2016.

[8] M.J. Duran, J. Prieto, F. Barrero and S. Toral, "Predictive current control of dual three-phase drives using restrained search techniques," *IEEE Trans. Ind. Electron.*, vol. 58, no. 8, pp. 3253–3263, 2011.

[9] F. Barrero, M.R. Arahal, R. Gregor, S. Toral and M.J. Duran, "One-step modulation predictive current control method for the asymmetrical dual three-phase induction machine," *IEEE Trans. Ind. Electron.*, vol. 56, no. 6, pp. 1974–1983, 2009.

[10] R. Gregor, F. Barrero, S. Toral, M.J. Duran, M.R. Arahal, J. Prieto and J.L. Mora, "Predictive-SVPWM current control method for asymmetrical dual three-phase induction motor drives," *IET Electric Power Appl.,* vol. 4, no. 1, pp. 26–34, 2010.

[11] F. Barrero, J. Prieto, E. Levi, R. Gregor, S. Toral, M.J. Duran and M. Jones, "An enhanced predictive current control method for asymmetrical six-phase motor drives," *IEEE Trans. Ind. Electron.*, vol. 58, no. 8, pp. 3242–3252, 2011.

[12] M.J. Duran, J. Riveros, F. Barrero, H. Guzman and J. Prieto, "Reduction of common-mode voltage in five-phase induction motor drives using predictive control techniques," *IEEE Trans. Ind. Appl.*, vol. 48, no. 6, pp. 2059–2067, 2012.

[13] C.S. Lim, E. Levi, M. Jones, N.A. Rahim and W.P. Hew, "FCS-MPC-based current control of a five-phase induction motor and its comparison with PI-PWM control," *IEEE Trans. Ind. Electron.*, vol. 61, no. 1, pp. 149–163, 2014.

[14] P. Alkorta, O. Barambones, J. Cortajarena and A. Zubizarreta, "Efficient multivariable generalized predictive control for sensorless induction motor drives," *IEEE Trans. Ind. Electron.*, vol. 61, no. 9, pp. 5126–5134, 2014.

[15] M. Habibullah and D.D.-C. Lu, "A speed-sensorless FS-PTC of induction motors using extended Kalman filters," *IEEE Trans. Ind. Electron.*, vol. 62, no. 11, pp. 6765–6778, 2015.

[16] C. Xia, M. Wang, Z. Song and T. Liu, "Robust model predictive current control of three-phase voltage source PWM rectifier with online disturbance observation," *IEEE Trans. Ind. Informat.*, vol. 8, no. 3, pp. 459–471, 2012.

[17] H. Liu and S. Li, "Speed control for PMSM servo system using predictive functional control and extended state observer," *IEEE Trans. Ind. Electron.*, vol. 59, no. 2, pp. 1171–1183, 2012.

[18] Y. Zhao and T. Lipo, "Space vector PWM control of dual three-phase induction machine using vector space decomposition," *IEEE Trans. Ind. Appl.*, vol. 31, no. 5, pp. 1100–1109, 1995.

[19] R. Mehra, "On the identification of variances and adaptive Kalman filtering," *IEEE Trans. Autom. Control*, vol. 15, no. 2, pp. 175–184, 1970.

[20] J. Kautsky, N. K. Nichols and P. Van Dooren, "Robust pole assignment in linear state feedback," *Inter. J. Control*, vol. 41, no. 5, pp. 1129–1155, 1985.

[21] J. Maes and J. Melkebeek, "Speed-sensorless direct torque control of induction motors using an adaptive flux observer," *IEEE Trans. Ind. Appl.*, vol. 36, no. 3, pp. 778–785, 2000.

[22] A. Yepes, J. Riveros, J. Doval–Gandoy, F. Barrero, O. Lopez, B. Bogado, M. Jones and E. Levi, "Parameter identification of multiphase induction machines with distributed windings – Part 1: sinusoidal excitation methods," *IEEE Trans. Energy Convers.*, vol. 27, no. 4, pp. 1056–1066, 2012.

[23] J. Riveros, A. Yepes, F. Barrero, J. Doval–Gandoy, B. Bogado, O. Lopez, M. Jones and E. Levi, "Parameter identification of multiphase induction machines with distributed windings – Part 2: time domain techniques," *IEEE Trans. Energy Convers.*, vol. 27, no. 4, pp. 1067–1077, 2012.

Jorge Rodas (S'08–M'12) received his B.Eng. degree in Electronic Engineering from the Universidad Nacional de Asunción (UNA), Paraguay, in 2009. He received his M.Sc. degrees from the University of Vigo, Spain, in 2012 and from the University of Seville, Spain, in 2013. In 2011, he joined the Laboratory of Power and Control System at the UNA, where he is currently an Associate Professor. He is a recipient of a scholarship from Fundación Carolina, Spain, for his Ph.D. studies.

Federico Barrero (M'04–SM'05) received the M.Sc. and Ph.D. degrees in Electrical and Electronic Engineering from the University of Seville, Spain, in 1992 and 1998, respectively. In 1992, he joined the Electronic Engineering Department at the University of Seville, where he is currently an Associate Professor. He received the Best Paper Awards from the IEEE Transactions on Industrial Electronics for 2009 and from the IET Electric Power Applications for 2010–2011.

Manuel R. Arahal (M'06) was born in Seville, Spain, in 1966. He received the M.Sc. and Ph.D. degrees in Industrial Engineering from the University of Seville, Spain, in 1991 and 1996, respectively. He is currently a Professor at the Systems Engineering and Automation Department at the University of Seville. He has been distinguished with the Best Paper Awards from the IEEE Transactions on Industrial Electronics for 2009, and from the IET Electric Power Applications for 2010–2011.

Cristina Martín was born in Seville, Spain, in 1989. She received the Industrial Engineer degree from the University of Málaga, Spain, in 2014. In 2015, she joined the Electronic Engineering Department of the University of Seville, where she is currently working toward the Ph.D. degree. Her current research interests include modeling and control of multiphase drives, microprocessor and DSP device systems, and electrical vehicles.

Raúl Gregor received the M.Sc. and Ph.D. degrees in Electrical and Electronic Engineering from the University of Seville, Spain, in 2008 and 2010, respectively. He is currently the Head of the Laboratory of Power and Control System of the National University of Asuncion, Paraguay. He received the Best Paper Awards from the IEEE Transactions on Industrial Electronics for 2009 and from the IET Electric Power Applications for 2010–2011.